

Aligning Individual and Collective Objectives in Multi-Agent Cooperation

Yang Li¹ Wenhao Zhang² Jianhong Wang¹ Shao Zhang² Yali Du³ Ying Wen² Wei Pan¹

Abstract

In the field of multi-agent learning, the challenge of mixed-motive cooperation is pronounced, given the inherent contradictions between individual and collective goals. Current research in this domain primarily focuses on incorporating domain knowledge into rewards or introducing additional mechanisms to foster cooperation. However, many of these methods suffer from the drawbacks of manual design costs and the lack of a theoretical grounding convergence procedure to the solution. To address this gap, we approach the mixed-motive game by modeling it as a differentiable game to study learning dynamics. We introduce a novel optimization method named *Altruistic Gradient Adjustment (AgA)* that employs gradient adjustments to novelly align individual and collective objectives. Furthermore, we provide theoretical proof that the selection of an appropriate alignment weight in AgA can accelerate convergence towards the desired solutions while effectively avoiding the undesired ones. The visualization of learning dynamics effectively demonstrates that AgA successfully achieves alignment between individual and collective objectives. Additionally, through evaluations conducted on established mixed-motive benchmarks such as the public good game, Cleanup, Harvest, and our modified mixed-motive SMAC environment, we validate AgA’s capability to facilitate altruistic and fair collaboration.

1. Introduction

Multi-agent cooperation primarily focuses on learning how to promote collaborative behavior in shared environments. Typically, research divides multi-agent cooperation into two prominent areas, pure-motive cooperation and mixed-motive cooperation (Du et al., 2023; McKee et al., 2020a). Re-

cent progress in cooperative Multi-Agent Reinforcement Learning (MARL) has primarily focused on addressing pure-motive cooperation, which also known as a common-payoff game, represents situations where individual goals fully align with collective objectives (Yu et al., 2022; Wang et al., 2020; Zhong et al., 2023; Li et al., 2024). Despite pure-motive cooperation, mixed-motive cooperation, which is typically defined by the imperfect alignment between individual and collective rationalities, is more common in real-world scenarios (Rapoport, 1974; McKee et al., 2020a).

Recent mixed-motive cooperative studies in MARL have largely employed hand-crafted designs to promote collaboration. Incorporating additional mechanisms to align objectives appears to be a popular avenue, including aspects such as reputation (Anastassacos et al., 2021), norms (Vinitsky et al., 2023), and contracts (Hughes et al., 2020). Another prevalent method draws on intrinsic motivation to align individual and collective objectives, augmenting altruistic collaboration by integrating heuristic knowledge into the incentive function. Conventionally, some works accumulate individual rewards with the group to cultivate altruistic conduct (Hostallero et al., 2020; Peysakhovich & Lerer, 2018; Apt & Schäfer, 2014). Furthermore, some studies derive more sophisticated preference signals from the rewards of other agents (Hughes et al., 2018; McKee et al., 2020a). Additionally, several approaches aim to learn the potential influences of an agent’s actions on others (Yang et al., 2020; Jaques et al., 2019; Lu et al., 2022). Most of these algorithms are highly dependent on carefully crafted designs, necessitating significant human expertise and detailed domain knowledge. However, they lack in-depth theoretical analysis concerning alignment and convergence.

In this work, we first present the differentiable mixed-motive game (DMG), premised on the assumption that the players’ loss functions are at least twice differentiable. The proposed formulation offers an efficient tool for analyzing the dynamics of gradient-based methods when optimizing mixed-motive objectives. Furthermore, we explore the optimization trajectories of simultaneous optimization methods and gradient adjustment methods (consensus optimization (Mescheder et al., 2017) and symplectic gradient adjustment (Letcher et al., 2019)) in the context of a two-player DMG, as shown in Fig. 1. First, we observe that gradient adjustment methods are ineffective in addressing

¹Department of Computer Science, University of Manchester, Manchester, UK ²Shanghai Jiao Tong University, Shanghai, China

³Department of Informatics, King’s College London, London, UK. Correspondence to: Ying Wen <ying.wen@sjtu.edu.cn>, Wei Pan <wei.pan@manchester.ac.uk>.

mixed-motive problems. These methods tend to prioritize stability at the expense of mitigating individual loss, which conflicts with the interests of individual participants (Chen et al., 2023). While simultaneous optimization with collective loss successfully enhances collective interests, it seems to neglect individual interests.

To address the issue, we propose an **Altruistic Gradient Adjustment (AgA)** optimization algorithm, designed to align individual and collective objectives from a gradient perspective. We provide a theoretical proof to suggest that appropriately choosing the sign of the alignment weight of the gradient terms could speed up the convergence of the AgA optimization strategy towards stable fixed point of collective objective while effectively bypassing unstable ones. The trajectory visualizations in Fig. 1, along with the sign selection ablation study trajectories presented in Fig. 3, serve to demonstrate successful alignment of objectives.

To further assess the effectiveness of our proposed AgA approach, we perform an assortment of experiments on a two-player public goods game and two sequential social dilemma games (Cleanup and Harvest) (Leibo et al., 2017). Given the relatively simple nature of these standard test scenarios used in mixed-motive cooperation contexts, we chose to modify the widely used SMAC environment (Samvelyan et al., 2019) to create a more complex mixed-motive cooperative setting. Evaluation based on various performance metrics including social welfare, equality, and win rate, suggests that the AgA approach surpasses the performance of baseline methods.

The contribution of the paper can be summarized as follows: (1) We introduce the differentiable mixed-motive game (DMG) and propose Altruistic Gradient Adjustment (AgA) algorithm to align individual and collective objectives from a gradient perspective. (2) We theoretically prove that careful selection of the alignment weight's sign can expedite convergence in AgA and effectively avoid unstable fixed points. (3) Visualizations based on a two-player DMG show that our method efficiently aligns individual and collective objectives. Further experiments conducted on mixed-motive testbeds and modified SMAC environments underscore the superior performance of our AgA method in several measurement metrics compared to baselines.

2. Related Work

Mixed-motive cooperation. Mixed-motive cooperation refers to scenarios where the group's objectives are sometimes aligned and at other times conflicted (Philip S. Gallo & McClintock, 1965). Recently, there has been a surge in academic interest in the Sequential Social Dilemma (SSD) (Leibo et al., 2017), which expands the concept from its roots in matrix games (Macy & Flache, 2002) to Markov

games. Prosocial (Peysakhovich & Lerer, 2018) improves collective performance by blending individual rewards to redraft the agent's overall utility. While PED-DQN enables agents to incrementally adjust their reward functions for enhanced collaborative action through inter-agent evaluative signal exchanges (Hostallero et al., 2020), Gifting directly reward other agents as part of action space (Lupu & Precup, 2020). Inequity aversion further integrates the concept into Markov games by adding envy (disadvantageous inequality) and guilt (advantageous inequality) rewards to the original individual rewards (Hughes et al., 2018). Simultaneously, Social Value Orientation (SVO) strategy introduces a unique shared rewards-based compensation approach, encouraging behavior modifications in line with interdependence theory (McKee et al., 2020b). The LIO strategy bypasses the need to modify extrinsic rewards by empowering an agent to directly influence its partner's actions (Yang et al., 2020). Meanwhile, other studies introduce new cooperative mechanisms such as incorporating a reputation model as an intrinsic reward (McKee et al., 2023). The CNM strategy delineates acceptable and unacceptable behaviors using classifiers as social norms, aiding agents to learn advantageous norms for improved returns per agent (Vinitsky et al., 2023). Despite these advances, many current studies lack both cost-efficiency in design and theoretical analysis of alignment and convergence. To address this, our study applies a gradient perspective to align goals and further investigates the learning dynamics of our proposed method.

Gradient-based Methods. Our proposed AgA is fundamentally a gradient adjustment methodology, making gradient-based optimization methods highly relevant to the context of this paper. Methods based on gradient have been developed to find stationary points, such as the Nash equilibrium or stable fixed points. Optimistic Mirror Descent leverages historical data to extrapolate subsequent gradients (Daskalakis et al., 2018), while Gidel et al. (2020) extends this concept by advocating averaging methodologies and variants of extrapolation techniques. Consensus gradient adjustment, or consensus optimization, is a technique that embeds a consensus agreement term within the gradient to ensure its convergence (Mescheder et al., 2017). Learning with Opponent-Learning Awareness (LOLA) utilizes information from other players to compute one player's anticipated learning steps (Foerster et al., 2018). Subsequently, Stable Opponent Shaping (SOS) (Letcher et al., 2021) and Consistent Opponent-Learning Awareness (COLA) (Willi et al., 2022) methods have enhanced the LOLA algorithm, targeting convergence assurance and inconsistency elimination, respectively. Symplectic Gradient Adjustment (SGA) alters the update direction towards the stable fixed points based on a novel decomposition of game dynamics (Baldazzi et al., 2018; Letcher et al., 2019). Recently, Learning to Play Games (L2PG) ensures convergence towards a sta-

ble fixed point by predicting updates to players' parameters derived from historical trajectories (Chen et al., 2023). However, these methods, while focusing on zero-sum or general sum games, could potentially act counter to their individual interests, as they may prioritize stability over minimizing personal loss. Our research specifically targets the mixed-motive setting with the aim of reconciling individual and collective objectives.

3. Preliminaries

Differential Game. The theory of differential games was initially proposed by Isaacs (1965), aiming to expand the scope of sequential game theory to encompass continuous-time scenarios. Through the lens of machine learning, we formalize the differential game, as shown in Definition 3.1.

Definition 3.1 (Differential Game (Balduzzi et al., 2018; Letcher et al., 2019)). *A differential game could be defined as a tuple $\{\mathcal{N}, \mathbf{w}, \ell\}$, where $\mathcal{N} = \{1, \dots, n\}$ delineates the assembly of players. The parameter set $\mathbf{w} = [\mathbf{w}_i]^n \in \mathbb{R}^d$ is defined, each with $\mathbf{w}_i \in \mathbb{R}^{d_i}$ and $d = \sum_{i=1}^n d_i$. Here, $\ell = \{\ell_i : \mathbb{R}^d \rightarrow \mathbb{R}\}_{i=1}^n$ represents the corresponding losses. These losses are assumed to be at least twice differential. Each player $i \in \mathcal{N}$ is equipped with a policy, parameterized by \mathbf{w}_i , aiming to minimize its individual loss ℓ_i .*

We rewrite the *simultaneous gradient* $\xi(\mathbf{w})$ of a differential game as $\xi(\mathbf{w}) = (\nabla_{\mathbf{w}_1} \ell_1, \dots, \nabla_{\mathbf{w}_n} \ell_n) \in \mathbb{R}^d$, which is the gradient of the losses with respect to the parameters of the respective players. Furthermore, *Hessian matrix* \mathbf{H} mentioned in a differential game is the Jacobian matrix of the simultaneous gradient.

The *learning dynamics* of differential game often refers to the process of sequential updates over \mathbf{w} . The *learning rule* for each player is defined as the operator, $\mathbf{w} \leftarrow \mathbf{w} - \gamma \xi$, where ξ is a feasible direction, and γ is a step size (learning rate) to determine the distance to move for each update.

Gradient Adjustment Optimization. The stable fixed point, a criterion initiated from stability theory, corresponds to the nature of local Nash equilibria (Balduzzi et al., 2018), as defined within the field of game theory. More specifically, a stable fixed point, exhibiting its stability (robustness) to minor perturbations from environments, making it applicable to many real-world scenarios. The concept of stable fixed point prevailing in general-sum and zero-sum games, is defined as follows.

Definition 3.2. *A point \mathbf{w}^* is a fixed point if $\xi(\mathbf{w}^*) = 0$. If $\mathbf{H}(\mathbf{w}^*) \succeq 0$ and $\mathbf{H}(\mathbf{w}^*)$ is invertible, the fixed point \mathbf{w}^* is called stable fixed point. If $\mathbf{H}(\mathbf{w}^*) \prec 0$, the point is called unstable.*

A naive idea to steer the dynamic towards convergence at stable fixed points involves minimizing $\frac{1}{2} \|\xi(\mathbf{w})\|^2$. Assum-

ing the Hessian $\mathbf{H}(\mathbf{w})$ is invertible, then $\nabla(\frac{1}{2} \|\xi(\mathbf{w})\|^2) = \mathbf{H}^T \xi = 0$ holds true if and only if $\xi = 0$. However, it could fail to converge to stable fixed point (Mescheder et al., 2017). Hence, the consensus optimization method has been proposed, incorporating gradient adjustment (Mescheder et al., 2017), shown as follows:

$$\tilde{\xi} = \xi + \lambda \cdot \nabla \frac{1}{2} \|\xi(\mathbf{w})\|^2 = \xi + \lambda \cdot \mathbf{H}^T \xi. \quad (1)$$

For simplicity, we will refer to the consensus gradient adjustment as *CGA*. While CGA proves effective in certain specific scenarios, such as two-player zero-sum games, it unfortunately falls short in general games (Balduzzi et al., 2018). To address this shortage, symplectic gradient adjustment (*SGA*) (Balduzzi et al., 2018; Letcher et al., 2019) is introduced to find the stable fixed point in general sum games, such that $\tilde{\xi} = \xi + \lambda \cdot \mathbf{A}^T \xi$. Herein, \mathbf{A} represents the antisymmetric component of the generalized Helmholtz decomposition of \mathbf{H} , $\mathbf{H}(\mathbf{w}) = \mathbf{S}(\mathbf{w}) + \mathbf{A}(\mathbf{w})$, where $\mathbf{S}(\mathbf{w})$ denotes the symmetric component. The hyperparameter λ is determined by the following formula: $\lambda = \text{sign}(\frac{1}{d} \langle \xi, \mathbf{H}^T \xi \rangle \langle \mathbf{A}^T \xi, \mathbf{H}^T \xi \rangle + \epsilon)$, where ϵ is a small positive number.

4. Method

4.1. Differentiable Mixed-motive Game

We first formulate the mixed-motive game as a differentiable game. Specifically, the *differentiable mixed-motive game (DMG)* is defined as a tuple $(\mathcal{N}, \mathbf{w}, \ell)$, where $\ell_i \in \ell$ is at least twice the differentiable loss function for the agent i . Differentiable losses exhibit the mixed motivation property: minimization of individual losses can result in a conflict between individuals or between individual and collective objectives (e.g., maximizing social welfare or beating opponents in basketball matches). The primary objective of DMG is to optimize the collective objective by minimizing collective loss, denoted as ℓ_c , while simultaneously taking into account the need to minimize individual objectives, represented by ℓ . Before delving into our interest alignment methods, let us first introduce some notations. We use $\xi_c(\mathbf{w})$ to refer the gradient of collective loss: $\xi_c(\mathbf{w}) = (\nabla_{\mathbf{w}_1} \ell_c, \dots, \nabla_{\mathbf{w}_n} \ell_c)$.

Nonetheless, direct optimization of individual or collective losses can lead to convergence issues and a mismatch between individual and collective interests. It is improbable that by minimizing only the individual loss of each agent, a collective minimum will be achieved (Leibo et al., 2017; McKee et al., 2020b). On the other hand, optimizing collective loss might produce improved collective outcomes, but at the risk of overlooking individual interests. This phenomenon is also demonstrated in Example 4.1. Furthermore, the local convergence of the gradient descent on singular col-

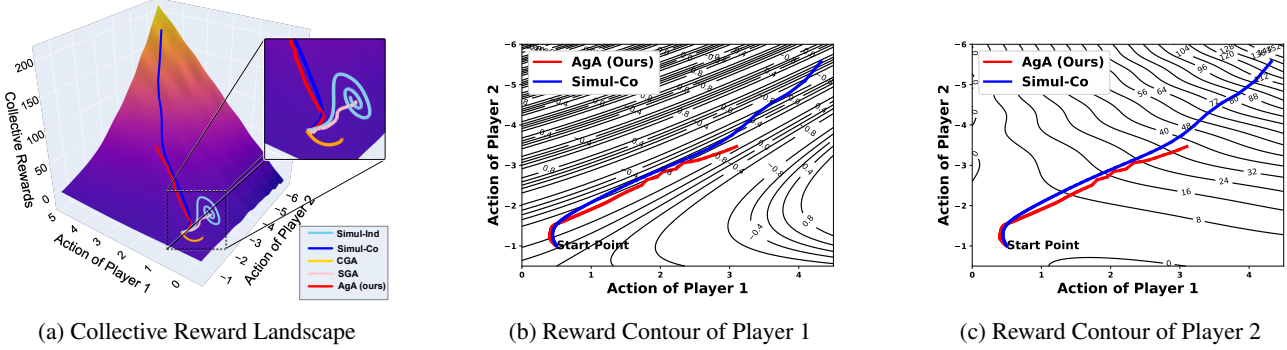


Figure 1. Trajectories of optimization in a two-player DMG (as delineated in Example 4.1). Fig. 1a displays the trajectories over the collective reward landscape - deeper orange equates to higher rewards. Remarkably, only Simul-Co and AgA make successful strides towards the social optimum. Fig. 1b and Fig. 1c delineate trajectories on the individual reward contour, underscoring Simul-Co’s neglect for Player 1’s interests even though it achieves higher rewards with fewer steps (65 steps versus 100 steps of AgA). Conversely, our AgA optimizes along the summit of Player 1’s reward while also maximizing the collective reward, demonstrating a *successful alignment*.

lective functions is not always guaranteed (Balduzzi et al., 2018). This also typifies the problem of credit assignment in MARL.

Alignment Dilemma in DMG. Here, we provide an example of a two-player differentiable mixed-motive game and the optimization results of the aforementioned methods.

Example 4.1. Consider a two-player DMG with $\ell_1(a_1, a_2) = -\sin(a_1 a_2 + a_2^2)$ and $\ell_2(a_1, a_2) = -[\cos(1 + a_1 - (1 + a_2)^2) + a_1 a_2^2]$. The rewards for the two players are the negation of their respective losses.

We provide a visual representation of optimization trajectories using a series of methods to investigate the learning dynamics involved in resolving the toy two-player differentiable mixed-motive game. In particular, we first implement simultaneous optimization of individual losses (Simul-Ind) with respect to each parameter, defined by the learning rule $\mathbf{w}_i = \mathbf{w}_i - \gamma \xi_i$, for $i \in \{1, 2\}$, where $\xi_i = \nabla_{\mathbf{w}_i} \ell_i$. Simultaneous optimization of collective loss (Simul-Co) replaces the individual gradient with the collective gradient ξ_c of collective loss $\ell_c = \ell_1 + \ell_2$. Furthermore, in order to investigate the learning dynamics of prevalent gradient modification optimization approaches such as SGA and CGA for the two-player differentiable mixed-motive game, we modify the learning rule by integrating the respective adjusted gradient as delineated in Section 3.

Fig. 1a shows the optimization paths on the collective reward landscapes, with every path starting from the front-bottom of the landscape. The collective reward is defined as social welfare, i.e., the sum of individual rewards. As shown in the figure, Simul-Ind, CGA, and SGA converge to unstable points or local maxima. Simul-Co effectively navigates towards the apex of the collective reward landscape as depicted in Fig. 1a. However, Simul-Co is ineffective in aligning individual and collective objectives, leading to the neglect of individual interests. As depicted in Fig. 1b, the

update trajectory navigates through the crests and troughs of Player 1’s reward contour. The trajectory suggests a disregard for Player 1’s preferences, signifying that the updates are predominantly driven by the overarching collective goal.

4.2. Altruistic Gradient Adjustment

In this section, we propose the alignment of individual and collective interests towards achieving stable fixed points of collective objectives within the context of mixed-motive cooperation. Revisit that the learning dynamics of simultaneous optimization on collective loss is given by $\mathbf{w} = \mathbf{w} - \gamma \xi_c$, where ξ_c represents the gradients of collective loss ℓ_c respectively, with respect to the parameters of each player $\mathbf{w}_i \in \mathbf{w}$. Although Simul-Co efficiently enhances collective performance, its shortcomings lie in not guaranteeing stable fixed points (Balduzzi et al., 2018) and overlooking individual interests as discussed in Example 4.1.

To tackle this challenge, we introduce the Altruistic Gradient Adjustment (AgA) method with the goal of aligning individual and collective objectives while seeking stable fixed points. Unlike existing gradient adjustment methods (Mescheder et al., 2017; Balduzzi et al., 2018; Letcher et al., 2019; Chen et al., 2023) that primarily focus on identifying the stable fixed points of individual losses, our proposed AgA method integrates the individual gradient into the collective gradient and ensures convergence to stable fixed points of the collective loss. Specifically, AgA is defined as follows.

Proposition 4.2 (Altruistic Gradient Adjustment). *Altruistic gradient adjustment (AgA) extends the gradient term in the learning dynamic as*

$$\tilde{\xi} := \xi_c + \lambda \xi_{adj} = \xi_c + \lambda (\xi + \mathbf{H}_c^T \xi_c), \quad (2)$$

where $\lambda \in \mathbb{R}$ is alignment parameter, $\lambda \xi_{adj}$ is called adjustment term. In ξ_{adj} , ξ_c and \mathbf{H}_c is the gradient vector and Hessian matrix of the game about collective loss.

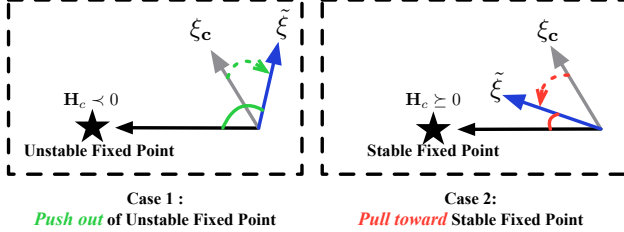


Figure 2. Illustration of Corollary 4.3. In case 1, within an unstable fixed point’s neighborhoods, an appropriate selection of the λ sign push AgA to evade the unstable fixed point and pull towards a stable fixed point in its neighborhoods as shown in case 2.

Note that the Hessian matrix \mathbf{H}_c is a symmetric matrix. To simplify the notation, we use $\nabla \mathcal{H}_c$ to denote the term $\nabla_{\mathbf{w}} \left(\frac{1}{2} \|\xi_c\|^2 \right)$, i.e., $\mathbf{H}_c^T \xi_c$.

Intuitively, AgA is designed to involve both collective and individual objectives, in order to harmonize the interests of individuals and the team. The alignment parameter λ adjusts the balance between the individual and the collective objective. Furthermore, we minimize $\mathcal{H}_c = \frac{1}{2} \|\xi_c\|^2$ to converge to a fixed point. This objective is reflected in the gradient term $\mathbf{H}_c^T \xi_c$ in $\tilde{\xi}$. Assuming that \mathbf{H}_c is invertible, we can deduce that $\nabla \mathcal{H}_c = \mathbf{H}_c^T \xi_c = 0$, if and only if $\xi_c = 0$. Therefore, minimizing \mathcal{H}_c will guarantee the convergence to a fixed point (Letcher et al., 2019).

Impact of the Sign of λ . While the modified AgA gradient introduces additional complexity, we theoretically demonstrate that an appropriate choice of the sign of λ ensures that the AgA gradient $\tilde{\xi}$ is attracted towards a stable fixed point. In contrast, when dealing with an unstable fixed point, AgA is pushed away the point.

Before we delve into the corollary of the sign selection for λ , we first establish some foundational definitions. The inner product of vectors \mathbf{a} and \mathbf{b} are denoted by $\langle \mathbf{a}, \mathbf{b} \rangle$. If the Hessian matrix \mathbf{H} is non-negative-definite, $\langle \xi_c, \nabla \mathcal{H} \rangle \geq 0$ for a non-zero ξ_c . Analogously, if \mathbf{H} is negative-definite, $\langle \xi_c, \nabla \mathcal{H} \rangle < 0$ for a non-zero ξ_c . Lastly, the angle between the two vectors \mathbf{a} and \mathbf{b} is denoted by $\theta(\mathbf{a}, \mathbf{b})$.

The following corollary states that AgA with a suitable sign of λ will bring the adjusted gradient $\tilde{\xi}$ point closer to a stable fixed point and escape from unstable fixed points.

Corollary 4.3. *If we let the sign of λ satisfy $\lambda \cdot \langle \xi_c, \nabla \mathcal{H}_c \rangle (\langle \xi, \nabla \mathcal{H}_c \rangle + \|\nabla \mathcal{H}_c\|^2) \geq 0$, the optimization process using the AgA method exhibit following attributes. Primarily, in neighborhood of fixed point of collective objective, if the point is stable ($\mathbf{H}_c \succeq 0$), the AgA gradient will be pulled toward this point, which means that $\theta(\tilde{\xi}, \nabla \mathcal{H}_c) \leq \theta(\xi_c, \nabla \mathcal{H}_c)$. On the other hand, if the point represents unstable equilibria where $\mathbf{H}_c \prec 0$, the AgA gradient will be pushed out of the point, indicating that $\theta(\tilde{\xi}, \nabla \mathcal{H}_c) \geq \theta(\xi_c, \nabla \mathcal{H}_c)$.*

The proof is provided in Appendix A. Fig. 2 presents a illus-

Algorithm 1 Altruistic Gradient Adjustment (AgA)

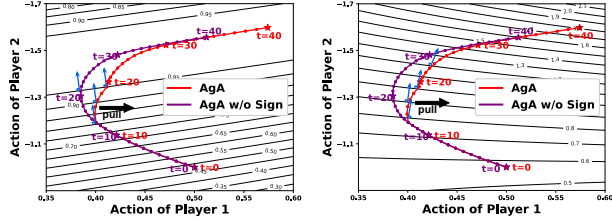
```

1: Input: individual losses  $\ell = [\ell_1, \dots, \ell_n]$ , collective loss  $\ell_c$ , parameters  $\mathbf{w} = [w_1, \dots, w_n]$ , magnitude of alignment parameter  $\lambda$ 
2:  $\xi \leftarrow [\text{grad}(\ell_i, \mathbf{w}_i) \text{ for } (\ell_i, \mathbf{w}_i) \in (\ell, \mathbf{w})]$ 
3:  $\xi_c \leftarrow [\text{grad}(\ell_c, \mathbf{w}_i) \text{ for } \mathbf{w}_i \in \mathbf{w}]$ 
4:  $\nabla \mathcal{H}_c \leftarrow [\text{grad}(\frac{1}{2} \|\xi_c\|^2, \mathbf{w}_i) \text{ for } \mathbf{w}_i \in \mathbf{w}]$ 
5:  $\lambda \leftarrow \lambda \times \text{sign} \left( \frac{1}{d} \langle \xi_c, \nabla \mathcal{H}_c \rangle (\langle \xi, \nabla \mathcal{H}_c \rangle + \|\nabla \mathcal{H}_c\|^2) \right)$ 
6: Output:  $\tilde{\xi} = \xi_c + \lambda(\xi + \nabla \mathcal{H}_c)$ 
    {Plug into any gradient descent optimizer}

```

trative visualization of Corollary 4.3. The figure depicts two scenarios: the neighborhoods of stable and unstable fixed point (denoted by a star), respectively. In the neighborhood of an unstable fixed point of the collective objective, as depicted in Case 1, our AaA gradient $\tilde{\xi}$ is pushed out of the region, resulting in a faster escape compared to the original collective gradient ξ_c . This behavior is exemplified by the green arrow. Conversely, Case 2 illustrates the scenario of a stable fixed point, wherein our AaA gradient $\tilde{\xi}$ is pulled towards the stable equilibrium, exemplified by the red arrow.

Implementation of MARL Algorithms with AgA. The concrete implementation of altruistic gradient adjustment is elaborated in Algorithm 1. AgA can be easily incorporated into any centralized training decentralized execution (CTDE) framework of MARL. In a typical CTDE framework, each agent, denoted as i , strives to learn a policy that employs local observations to prompt a distribution over personal actions. The unique characteristic during the centralized learning phase is that agents gain supplementary information from their peers that is inaccessible during the execution stage. Furthermore, a centralized critic often operates in tandem in CTDE settings, leveraging shared information and evaluating individual agent policies’ potency. To incorporate our proposed AgA algorithm into CTDE frameworks, supplementary reward exchanges between agents are required, offering the essential inputs for Algorithm 1. The individual losses are calculated from individual rewards conforming to established MARL algorithm framework, such as IPPO (de Witt et al., 2020) or MAPPO (Yu et al., 2022). Here, the collective loss ℓ_c is calculated according to individual rewards; for example, it could be a sum of individual rewards or an elementary transformation thereof. Furthermore, the AgA algorithm requires a magnitude value of the alignment parameter λ , which should be a positive entity. The sign of λ is then calculated in line 5 of Algorithm 1 and is based on each gradient component calculated in lines 2-4. Subsequently, the algorithm produces the adjusted gradient $\tilde{\xi}$. $\tilde{\xi}$ is then distributed across each corresponding parameter, and optimization is carried out using a suitable optimizer such as Adam optimizer (Kingma & Ba, 2015).



(a) Reward Contour of Player 1 (b) Reward Contour of Player 2

Figure 3. The comparison between AgA (shown in red) and AgA without sign alignment (AgA w/o Sign, in purple) trajectories spans 40 steps, marked at every tenth step. Norm gradients are represented with blue arrows. Starting from the 14th step, sign alignment pull the update direction. Consequently, AgA is about 6 steps ahead of AgA w/o Sign at the trajectory’s end.

4.3. Alignment Efficiency of AgA: A Toy Experiment

To address the two-player DMG as outlined in Example 4.1, we incorporate the AgA method into the fundamental gradient descent algorithm. The findings reveal that the AgA method is effective in facilitating the alignment of objectives. The optimization trajectories in both the collective reward landscape and the individual player reward contour are represented in Fig. 1a, Fig. 1b, and Fig. 1c, with brighter colors reflecting higher collective rewards. In contrast to the objective misalignment exhibited by Simul-Co, AgA successfully aligns the agents’ interests, as evidenced in Fig. 1b and Fig 1c. Fig. 1b depicts the trajectory of AgA meticulously carving its course along the summit of the individual reward contour. Furthermore, AgA is also shown to improve the reward of Player 2 (as shown in Fig. 1c), despite a convergence rate slower than that of Simul-Co. Evidently, the trajectory of AgA (as depicted in Fig. 1b) takes 100 steps, whereas Simul-Co takes 65 steps.

In addition, Fig. 3 presents a critical comparison between the trajectories of AgA (in red) and AgA without sign alignment (AgA w/o Sign, depicted in purple), as outlined in Corollary 4.3. This side-by-side comparison covers 40 steps and features highlighted points every tenth step. It provides a visual illustration of the efficiency introduced by sign alignment starting from the 14th step in the trajectories of AgA and AgA without sign alignment. Remarkably, norm gradients are represented by blue arrows, indicating the direction of the fastest updates. As depicted in the figure, AgA with sign selection is aligned towards the fastest update direction, resulting in AgA progressing approximately 6 steps ahead of AgA without Sign at the end of the trajectory.

5. Experiments

In this section, we conduct a series of experiments to verify the AgA algorithm. First, we provide an overview of the experimental settings and clarify the evaluation metrics employed.

Metrics	Algorithms					
	Simul-Ind	CGA	SGA	SVO	Simul-Co	AgA
r_1	1.13	1.16	1.18	1.10	1.43	1.46
r_2	1.18	1.15	1.14	1.06	1.38	1.45
SW	2.32	2.31	2.31	2.16	2.81	2.90
E	0.92	0.93	0.92	0.93	0.94	0.96

Table 1. The comparison of the average individual rewards (denoted as r_1, r_2), social welfare (denoted as SW) and equality metric (denoted as E). Each value is the mean of 50 random runs.

Baselines and Evaluation Metrics. A comparison of experiments involves specific baselines such as simultaneous optimization with individual and collective losses (abbreviated as Simul-Ind and Siml-Co), CGA (Mescheder et al., 2017), SGA (Balduzzi et al., 2018) and SVO (McKee et al., 2020a). In the two-player public goods game experiment, these techniques are simply integrated into the basic gradient ascent algorithm, whereas, for more intricate settings like Cleanup, Harvest (Leibo et al., 2017), and SMAC (Samvelyan et al., 2019), these baselines are infused within various RL algorithms. Detailed operations for implementing these RL algorithms are further elucidated in their respective sections.

We assess collaborative performance in mixed-motive games using a three-tier approach. Primarily, we employ social welfare to gauge overall team performance. Next, an equality metric is introduced to scrutinize fairness in environments such as Cleanup and Harvest. Lastly, the probability of victory against opposition in an SMAC framework determines the probability of the team’s success. **Social Welfare** is a commonly accepted metric for evaluating the performance of mixed motivation cooperation, representing the total episodic rewards earned by all agents as $SW = \sum_{i=1}^n r_i$. Social welfare lacks the ability to analyze teamwork in mixed cooperative-competitive contexts. Here, we use the average **Win Rate** against the built-in computer AI bot in SMAC to assess algorithmic performance. We also involve the **Equality** due to the measures like social welfare and win rate are limited to a general performance evaluation, ignoring individual interest. Therefore, the Gini coefficient, originally intended as an income equality measure (David, 1968), has been modified to assess reward equality in cooperative AI settings. This study utilizes an expedited Gini coefficient calculation method, with an associated equality metric E , formulated as $E := 1 - G$. Each individual’s rewards are arranged in ascending order to create a new payoff vector \mathbf{p} , and the Gini coefficient is computed as $G = \frac{2}{n^2 \bar{p}} \sum_{i=1}^n i(p_i - \bar{p})$, followed by $E = 1 - G$. Here, \bar{p} denotes the mean of the ranked payoff vector \mathbf{p} and n signifies the total number of players. A larger E value implies greater equality.

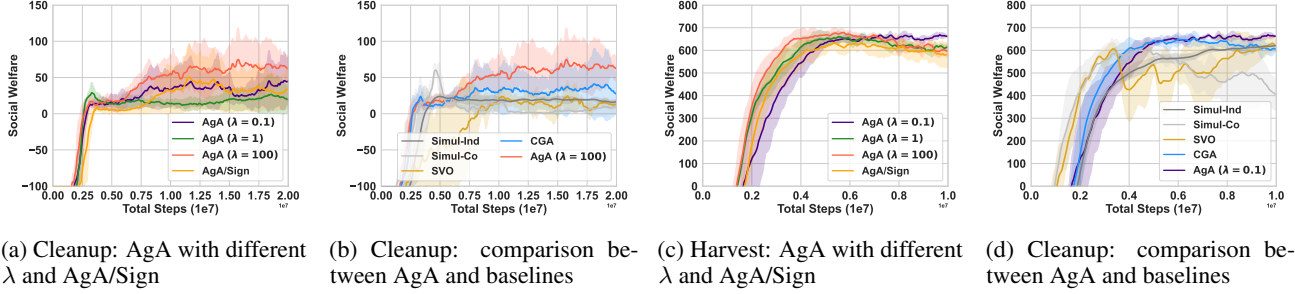


Figure 4. Comparison of Episodic Social Welfare: our proposed AgA methods along with baselines on Cleanup (figure a and b) and Harvest (figure c and d) tasks. Figure (a) and (c) provide an illustration of varying alignment parameter λ values in AgA, as well as AgA sans sign selection (AgA/Sign), as applied to Cleanup and Harvest tasks respectively. Subfigures (b) and (d) exhibit the social welfare obtained by AgA utilizing the optimal λ value, in comparison to those secured by Simul-Ind, Simul-Co, CGA, SGA and SVO. Bold lines represent the average of the social welfare across three seeds, with the encompassing shaded areas denoting the standard deviation.

5.1. Two-Player Public Goods Game

A two-player Public Goods matrix game \mathcal{G} is widely utilized to study cooperation in social dilemmas. The game involves players $\{1, 2\}$ with parameters $\{w_1, w_2\}$ and payoffs $\{p_1, p_2\}$. The social welfare, denoted as $SW = p_1 + p_2$. Each player, i.e., $i \in \{1, 2\}$, contributes an amount a_i within a budgeted range $[0, b]$, and the host evenly distributes these contributions as $\frac{c}{2}(a_1 + a_2)$, where $1 < c \leq 2$. Consequently, each player's payoff $p_i(a_1, a_2)$ is estimated as $b - a_i + \frac{c}{2}(a_1 + a_2)$. In our experiments, we set the budget b to 1 and weight c to 1.5, with the Nash equilibrium of game at $(0, 0)$.

Results. Table 1 compares averindvidual rewards, social welfare, and the equality metric sourced from 50 random runs, each capped at 100 steps. The rows r_1, r_2 and SW represent the rewards accrued by each individual player and the collective group respectively. Row E denotes the equality metric. The table reveals that AgA surpasses benchmark methods in individual rewards and social welfare, and equality metric. The social optimum of the game is at coordinates $(1, 1)$, which corresponds to a maximum achievable social welfare of 3. Among all the algorithms, AgA achieves the closest social welfare score to this optimum, with a value of 2.90. In addition, AgA demonstrates the highest level of equality, with a score of 0.96, when compared to the baseline algorithms. Additionally, Fig. 6 in Appendix B visualizes the action distributions of these methods, demonstrating convergence points, further supporting that AgA converges more efficiently towards the social optimum.

5.2. Sequential Social Dilemma: Cleanup and Harvest

We conduct experiments in sequential social dilemma environments with a group size of five namely, Harvest and Cleanup (Hughes et al., 2018). In Cleanup, the agents primarily derive rewards from harvesting apples in a nearby orchard, which is contingent upon river pollution levels. If

Envs	Metrics	Algorithms				
		Simul-Ind	Simul-Co	SVO	CGA	AgA
Cleanup	SW	24.86	72.02	27.30	44.23	83.90
	E	0.97	0.88	0.85	0.91	0.95
Harvest	SW	623.13	625.80	638.95	667.37	683.42
	E	0.97	0.96	0.97	0.98	0.98

Table 2. The highest social welfare achieved throughout training along with the corresponding equality metric. The foremost row for each environment reflects the best social welfare, while the second row indicates the associated equality metric.

negligence towards the escalating pollution levels surpasses a threshold, apple growth ceases, hence leading to a conflict of interest between obtaining individual rewards and safeguarding joint welfare. Harvest's premise, on the other hand, involves agents receiving rewards by gathering apples, whereby optimal apple regrowth is dependent on the presence of adjacent apples. A collective dilemma appears when rampant harvesting reduces the apple regeneration rate, thus decrementing overall team rewards. Simul-Ind, Simul-Co, CGA, and SVO are benchmarked against our AgA methodology in our experiments. The implementation of the Simul-Ind algorithm is based on the IPPO algorithm (de Witt et al., 2020), with all other strategies leveraging the shared parameters of the IPPO algorithm as well. The joint reward formula used for the calculation of collective loss for Simul-Co, CGA, and AgAs is designed to promote both improved collective performance and equitable behavior among agents, i.e., $\sum_i (r_i - \alpha(1 - \text{actan}(\frac{\sum_{j:j \neq i} r_j}{r_i})))$ with constant α . More detailed information on these environments and algorithm execution can be found in Appendix C.1.

Results. Fig. 4a and Fig. 4c present the average episodic social welfare comparison of the AgA algorithm and AgA/Sign, excluding the sign selection (Corollary 4.3). These figures also highlight the effect of varying the alignment parameter λ . The prescribed λ values for AgA/Sign is 100 for Cleanup and 0.1 for Harvest, resulting in the best performance for each. Failing to select signs in AgA/Sign leads

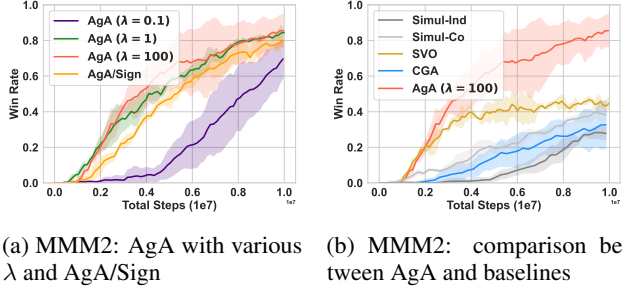


Figure 5. The comparison of win rates on the mixed-motive MMM2 map of SMAC. The left figure shows results of varying alignment parameter λ values in AgA, as well as AgA sans sign selection (AgA/Sign). The right figure compare the win rate of AgA ($\lambda = 100$) with baselines. The bold lines illustrate the mean of the win rate over 3 seeds, while the encompassing shaded regions depict the standard deviation.

to poorer collective results. Fig. 4b and Fig. 4d compare the social welfare achieved by AgA, with the optimal λ value, with baseline methods. Here, AgA ($\lambda = 100$) in Cleanup and AgA ($\lambda = 0.1$) in Harvest surpass the benchmark methods for the majority of the training process. Table 2 presents the peak social welfare achieved during training alongside the equality metric. For simplicity, the AgA column denotes the respective optimal λ for each scenario. In Cleanup, AgA surpasses the second-best method, Simul-Co, by over 10 points. However, although Simul-Ind shows superior equality performance, it delivers the lowest social welfare. Contrarily, AgA achieves a satisfactory balance between equity and team performance. Analogous conclusions apply to the Harvest, where AgA outperforms baselines in social welfare and equality.

5.3. Mixed-motive SMAC

Despite their widespread use in the study of mixed-motive games, sequential social dilemma games can be relatively simplistic compared to other testbeds in the field of MARL, particularly when considering real-world scenarios. Cooperative Multi-Agent Reinforcement Learning often adopts more intricate environments such as SMAC (Samvelyan et al., 2019). In this game environment, agents must collaborate to defeat their opponents. We modify the MMM2 map from SMAC as a mixed-motive testbed. Here, agents command various game entities confronting opposing forces. Unlike the original StarCraft II game’s team-oriented architecture, we instill individual interests in each agent to enhance mixed-motive characteristics. Reward mechanisms have been modified such that an agent’s individual reward aligns with the damage it inflicts on the enemy, replacing the standard practice of distributing total damage across all agents. Penalties for agent removal also reinforce self-preservation, accentuating inherent agent selfishness. The experimental implementation utilizes the IPPO algo-

rithm (de Witt et al., 2020) for Simul-Ind, while employing the MAPPO framework (Yu et al., 2022) for Simul-Co, SVO, CGA, and AgA. More details can be found in Appendix C.2.

Results. Fig. 5a compares average win rates for various λ parameters in AgA, also encompassing AgA without sign selection, as stated in Corollary 4.3. The results suggest comparable performance for $\lambda = 1$ and 100, with a lower value of 0.1 trailing noticeably. Notably, AgA with $\lambda = 0.1$ underperforms, even when contrasted with AgA’s ablation study. Fig. 5b benchmarks the win rate for AgA ($\lambda = 100$) against Simul-Ind, Simul-Co, CGA, and SVO. Within this context, Simul-Ind, implemented via IPPO, struggles with the mixed-motive MMM2 task. Impressively, our AgA ($\lambda = 100$) method achieves a win rate peak of 0.85 (standard deviation of 0.09), significantly outperforming the SVO method that only nets 44.55.

6. Conclusion

In this paper, we propose AgA, an gradient adjustment method, specifically designed to align individual and collective objectives within mixed-motive cooperation scenarios. To materialize this, we first model the mixed-motive game as a differentiable game, thereby facilitating the analysis of learning dynamics. Thereafter, we analyze the optimization paths in a toy differentiable mixed-motive game. We reveal that optimization techniques that heavily rely on collective loss suffer from inherent limitations. These approaches often overlook individual preferences, and existing gradient adjustment methods are inadequate for addressing mixed-motive cooperation challenges. Our AgA strategy efficiently bridges the gap between individual and collective objectives. The optimization paths further support our theoretical claims by demonstrating that careful selection of the sign of the alignment weight enables convergence towards stable fixed points while escaping unstable ones. Comprehensive experiments conducted on mixed-motive testbeds and modified SMAC environments provide further evidence of the superior performance of AgA. It consistently outperforms existing baselines across multiple evaluation metrics.

Limitations and Future Work. The experiments conducted in this study were confined to a single map of the SMAC environment. Our future objectives include investigating the mixed-motive cooperative mechanism in real-world scenarios and developing a more complex mixed-motive testbed. In this paper, while we strive to align the objectives of both individuals and the collective, our primary objective is to converge towards a stable equilibrium of the collective objective. For future research, we intend to broaden our comprehension of how individual objectives interact in mixed-motive games, placing a greater emphasis on understanding their dynamics in mixed-motive cooperation.

Impact Statements

This paper presents a novel approach in the field of multi-agent learning, aimed at advancing collaborations with mixed motivations. The proposed framework addresses a fundamental challenge in machine learning, wherein agents with diverse objectives are required to cooperate to achieve collective goals. The work described in this paper holds significant potential for various societal applications. By enabling effective cooperation among agents with different motivations, our approach can be leveraged in domains such as games, autonomous systems, smart cities, and decentralized resource allocation. Such advancements have numerous societal consequences, including improved efficiency in transportation systems, optimized resource allocation in energy grids, and enhanced decision-making in complex multi-agent environments. Furthermore, our findings contribute to the broader field of machine learning by offering insights into managing mixed-motivation scenarios. Consequently, our work paves the way for future research and innovation, driving progress in multi-agent learning and its applications across various domains.

References

- Anastassacos, N., García, J., Hailes, S., and Musolesi, M. Cooperation and reputation dynamics with reinforcement learning. In Dignum, F., Lomuscio, A., Endriss, U., and Nowé, A. (eds.), *AAMAS '21: 20th International Conference on Autonomous Agents and Multiagent Systems, Virtual Event, United Kingdom, May 3-7, 2021*, pp. 115–123. ACM, 2021. doi: 10.5555/3463952.3463972. URL <https://www.ifaamas.org/Proceedings/aamas2021/pdfs/p115.pdf>.
- Apt, K. R. and Schäfer, G. Selfishness level of strategic games. *J. Artif. Int. Res.*, 49(1):207–240, jan 2014. ISSN 1076-9757.
- Balduzzi, D., Racaniere, S., Martens, J., Foerster, J., Tuyls, K., and Graepel, T. The mechanics of n-player differentiable games. In *International Conference on Machine Learning*, pp. 354–363. PMLR, 2018.
- Chen, X., Vadovi, N., Chen, T., and Wang, Z. Learning to optimize differentiable games. In Krause, A., Brunskill, E., Cho, K., Engelhardt, B., Sabato, S., and Scarlett, J. (eds.), *Proceedings of the 40th International Conference on Machine Learning*, volume 202 of *Proceedings of Machine Learning Research*, pp. 5036–5051. PMLR, 23–29 Jul 2023. URL <https://proceedings.mlr.press/v202/chen23ab.html>.
- Daskalakis, C., Ilyas, A., Syrgkanis, V., and Zeng, H. Training gans with optimism, 2018.
- David, H. A. Gini's mean difference rediscovered. *Biometrika*, 55(3):573–575, 1968. ISSN 00063444. URL <http://www.jstor.org/stable/2334264>.
- de Witt, C. S., Gupta, T., Makoviichuk, D., Makoviychuk, V., Torr, P. H. S., Sun, M., and Whiteson, S. Is independent learning all you need in the starcraft multi-agent challenge? *CoRR*, abs/2011.09533, 2020. URL <https://arxiv.org/abs/2011.09533>.
- Du, Y., Leibo, J. Z., Islam, U., Willis, R., and Sunehag, P. A review of cooperation in multi-agent learning, 2023.
- Foerster, J. N., Chen, R. Y., Al-Shedivat, M., Whiteson, S., Abbeel, P., and Mordatch, I. Learning with opponent-learning awareness, 2018.
- Gidel, G., Berard, H., Vignoud, G., Vincent, P., and Lacoste-Julien, S. A variational inequality perspective on generative adversarial networks, 2020.
- Hostallero, D. E., Kim, D., Moon, S., Son, K., Kang, W. J., and Yi, Y. Inducing cooperation through reward reshaping based on peer evaluations in deep multi-agent reinforcement learning. In Seghrouchni, A. E. F., Sukthankar, G., An, B., and Yorke-Smith, N. (eds.), *Proceedings of the 19th International Conference on Autonomous Agents and Multiagent Systems, AAMAS '20, Auckland, New Zealand, May 9–13, 2020*, pp. 520–528. International Foundation for Autonomous Agents and Multiagent Systems, 2020. doi: 10.5555/3398761.3398825. URL <https://dl.acm.org/doi/10.5555/3398761.3398825>.
- Hughes, E., Leibo, J. Z., Phillips, M., Tuyls, K., Duéñez-Guzmán, E. A., Castañeda, A. G., Dunning, I., Zhu, T., McKee, K. R., Koster, R., Roff, H., and Graepel, T. Inequity aversion improves cooperation in intertemporal social dilemmas. In Bengio, S., Wallach, H. M., Larochelle, H., Grauman, K., Cesa-Bianchi, N., and Garnett, R. (eds.), *Advances in Neural Information Processing Systems 31: Annual Conference on Neural Information Processing Systems 2018, NeurIPS 2018, December 3–8, 2018, Montréal, Canada*, pp. 3330–3340, 2018. URL <https://proceedings.neurips.cc/paper/2018/hash/7fea637fd6d02b8f0adf6f7dc36aed93-Abstract.html>.
- Hughes, E., Anthony, T. W., Eccles, T., Leibo, J. Z., Balduzzi, D., and Bachrach, Y. Learning to resolve alliance dilemmas in many-player zero-sum games. *CoRR*, abs/2003.00799, 2020. URL <https://arxiv.org/abs/2003.00799>.
- Isaacs, R. *Differential Games: A Mathematical Theory with Applications to Warfare and Pursuit, Control and Optimization*. Dover books on mathematics. Wiley,

1965. ISBN 9780471428602. URL <https://books.google.co.uk/books?id=gt1QAAAAMAAJ>.
- Jaques, N., Lazaridou, A., Hughes, E., Gulcehre, C., Ortega, P., Strouse, D., Leibo, J. Z., and De Freitas, N. Social influence as intrinsic motivation for multi-agent deep reinforcement learning. In *International conference on machine learning*, pp. 3040–3049. PMLR, 2019.
- Kingma, D. P. and Ba, J. Adam: A method for stochastic optimization. In Bengio, Y. and LeCun, Y. (eds.), *3rd International Conference on Learning Representations, ICLR 2015, San Diego, CA, USA, May 7-9, 2015, Conference Track Proceedings*, 2015. URL <http://arxiv.org/abs/1412.6980>.
- Leibo, J. Z., Zambaldi, V. F., Lanctot, M., Marecki, J., and Graepel, T. Multi-agent reinforcement learning in sequential social dilemmas. *CoRR*, abs/1702.03037, 2017. URL <http://arxiv.org/abs/1702.03037>.
- Letcher, A., Balduzzi, D., Racanière, S., Martens, J., Foerster, J., Tuyls, K., and Graepel, T. Differentiable game mechanics. *Journal of Machine Learning Research*, 20(84):1–40, 2019. URL <http://jmlr.org/papers/v20/19-008.html>.
- Letcher, A., Foerster, J., Balduzzi, D., Rocktäschel, T., and Whiteson, S. Stable opponent shaping in differentiable games, 2021.
- Li, Y., Zhang, S., Sun, J., Zhang, W., Du, Y., Wen, Y., Wang, X., and Pan, W. Tackling cooperative incompatibility for zero-shot human-ai coordination, 2024.
- Lu, C., Willi, T., de Witt, C. A. S., and Foerster, J. N. Model-free opponent shaping. In Chaudhuri, K., Jegelka, S., Song, L., Szepesvári, C., Niu, G., and Sabato, S. (eds.), *International Conference on Machine Learning, ICML 2022, 17-23 July 2022, Baltimore, Maryland, USA*, volume 162 of *Proceedings of Machine Learning Research*, pp. 14398–14411. PMLR, 2022. URL <https://proceedings.mlr.press/v162/lu22d.html>.
- Lupu, A. and Precup, D. Gifting in multi-agent reinforcement learning. In *Proceedings of the 19th International Conference on autonomous agents and multiagent systems*, pp. 789–797, 2020.
- Macy, D. and Flache, A. Learning dynamics in social dilemmas. *Proceedings of the National Academy of Sciences of the United States of America*, 99 Suppl 3:7229–36, 06 2002. doi: 10.1073/pnas.092080099.
- McKee, K. R., Gemp, I., McWilliams, B., Duéñez-Guzmán, E. A., Hughes, E., and Leibo, J. Z. Social diversity and social preferences in mixed-motive reinforcement learning. In Seghrouchni, A. E. F., Sukthankar, G., An, B., and Yorke-Smith, N. (eds.), *Proceedings of the 19th International Conference on Autonomous Agents and Multiagent Systems, AAMAS '20, Auckland, New Zealand, May 9-13, 2020*, pp. 869–877. International Foundation for Autonomous Agents and Multiagent Systems, 2020a. doi: 10.5555/3398761.3398863. URL <https://dl.acm.org/doi/10.5555/3398761.3398863>.
- McKee, K. R., Gemp, I., McWilliams, B., Duéñez-Guzmán, E. A., Hughes, E., and Leibo, J. Z. Social diversity and social preferences in mixed-motive reinforcement learning, 2020b.
- McKee, K. R., Hughes, E., Zhu, T. O., Chadwick, M. J., Koster, R., Castaneda, A. G., Beattie, C., Graepel, T., Botvinick, M., and Leibo, J. Z. A multi-agent reinforcement learning model of reputation and cooperation in human groups, 2023.
- Mescheder, L. M., Nowozin, S., and Geiger, A. The numerics of gans. In Guyon, I., von Luxburg, U., Bengio, S., Wallach, H. M., Fergus, R., Vishwanathan, S. V. N., and Garnett, R. (eds.), *Advances in Neural Information Processing Systems 30: Annual Conference on Neural Information Processing Systems 2017, December 4-9, 2017, Long Beach, CA, USA*, pp. 1825–1835, 2017. URL <https://proceedings.neurips.cc/paper/2017/hash/4588e674d3f0faf985047d4c3f13ed0d-Abstract.html>.
- Peysakhovich, A. and Lerer, A. Prosocial learning agents solve generalized stag hunts better than selfish ones. In André, E., Koenig, S., Dastani, M., and Sukthankar, G. (eds.), *Proceedings of the 17th International Conference on Autonomous Agents and MultiAgent Systems, AAMAS 2018, Stockholm, Sweden, July 10-15, 2018*, pp. 2043–2044. International Foundation for Autonomous Agents and Multiagent Systems Richland, SC, USA / ACM, 2018. URL <http://dl.acm.org/citation.cfm?id=3238065>.
- Philip S. Gallo, J. and McClintock, C. G. Cooperative and competitive behavior in mixed-motive games. *Journal of Conflict Resolution*, 9(1):68–78, 1965. doi: 10.1177/002200276500900106. URL <https://doi.org/10.1177/002200276500900106>.
- Raffin, A., Hill, A., Gleave, A., Kanervisto, A., Ernestus, M., and Dormann, N. Stable-baselines3: Reliable reinforcement learning implementations. *Journal of Machine Learning Research*, 22(268):1–8, 2021. URL <http://jmlr.org/papers/v22/20-1364.html>.
- Rapoport, A. Prisoner’s dilemma—recollections and observations. In *Game Theory as a Theory of a Conflict Resolution*, pp. 17–34. Springer, 1974.

- Samvelyan, M., Rashid, T., de Witt, C. S., Farquhar, G., Nardelli, N., Rudner, T. G. J., Hung, C., Torr, P. H. S., Foerster, J. N., and Whiteson, S. The starcraft multi-agent challenge. In Elkind, E., Veloso, M., Agmon, N., and Taylor, M. E. (eds.), *Proceedings of the 18th International Conference on Autonomous Agents and MultiAgent Systems, AAMAS '19, Montreal, QC, Canada, May 13-17, 2019*, pp. 2186–2188. International Foundation for Autonomous Agents and Multiagent Systems, 2019. URL <http://dl.acm.org/citation.cfm?id=3332052>.
- Vinitsky, E., Jaques, N., Leibo, J., Castenada, A., and Hughes, E. An open source implementation of sequential social dilemma games. https://github.com/eugenevinitsky/sequential_social_dilemma_games/issues/182, 2019. GitHub repository.
- Vinitsky, E., Köster, R., Agapiou, J. P., Duéñez-Guzmán, E. A., Vezhnevets, A. S., and Leibo, J. Z. Eugene2023collectiveized multi-agent settings. *Collective Intelligence*, 2(2):26339137231162025, 2023. doi: 10.1177/26339137231162025. URL <https://doi.org/10.1177/26339137231162025>.
- Wang, J., Zhang, Y., Kim, T., and Gu, Y. Shapley q-value: A local reward approach to solve global reward games. In *The Thirty-Fourth AAAI Conference on Artificial Intelligence, AAAI 2020, The Thirty-Second Innovative Applications of Artificial Intelligence Conference, IAAI 2020, The Tenth AAAI Symposium on Educational Advances in Artificial Intelligence, EAAI 2020, New York, NY, USA, February 7-12, 2020*, pp. 7285–7292. AAAI Press, 2020. doi: 10.1609/AAAI.V34I05.6220. URL <https://doi.org/10.1609/aaai.v34i05.6220>.
- Willi, T., Letcher, A. H., Treutlein, J., and Foerster, J. COLA: Consistent learning with opponent-learning awareness. In Chaudhuri, K., Jegelka, S., Song, L., Szepesvari, C., Niu, G., and Sabato, S. (eds.), *Proceedings of the 39th International Conference on Machine Learning*, volume 162 of *Proceedings of Machine Learning Research*, pp. 23804–23831. PMLR, 17–23 Jul 2022. URL <https://proceedings.mlr.press/v162/willi22a.html>.
- Yang, J., Li, A., Farajtabar, M., Sunehag, P., Hughes, E., and Zha, H. Learning to incentivize other learning agents. *Advances in Neural Information Processing Systems*, 33: 15208–15219, 2020.
- Yu, C., Velu, A., Vinitsky, E., Gao, J., Wang, Y., Bayen, A. M., and Wu, Y. The surprising effectiveness of PPO in cooperative multi-agent games. In *NeurIPS*, 2022.
- Zhong, Y., Kuba, J. G., Hu, S., Ji, J., and Yang, Y. Heterogeneous-agent reinforcement learning, 2023.

A. Proof of Corollary 4.3

Corollary 4.3. *If we let the sign of λ satisfy $\lambda \cdot \langle \xi_c, \nabla \mathcal{H}_c \rangle (\langle \xi, \nabla \mathcal{H}_c \rangle + \|\nabla \mathcal{H}_c\|^2) \geq 0$, the optimization process using the AgA method exhibit following attributes. Primarily, in neighborhood of fixed point of collective objective, if the point is stable ($\mathbf{H}_c \succeq 0$), the AgA gradient will be pulled toward this point, which means that $\theta(\tilde{\xi}, \nabla \mathcal{H}_c) \leq \theta(\xi_c, \nabla \mathcal{H}_c)$. On the other hand, if the point represents unstable equilibria where $\mathbf{H}_c \prec 0$, the AgA gradient will be pushed out of the point, indicating that $\theta(\tilde{\xi}, \nabla \mathcal{H}_c) \geq \theta(\xi_c, \nabla \mathcal{H}_c)$.*

Proof. Prior to embarking on the elucidation of the corollary's proof, it is essential to first introduce relevant notations and the foundational concepts. Take note of the notation $\theta(\mathbf{a}, \mathbf{b})$, which symbolizes the angular measure between two vectors. Furthermore, we write $\theta_\lambda(\tilde{\xi}, \mathbf{w})$ to represent the angular measure between AgA gradient $\tilde{\xi}$ and a reference update direction \mathbf{w} . For simplicity, we use $\mathbf{u} = \mathbf{u} + \lambda \mathbf{v}$ to denote the AgA gradient $\tilde{\xi} = \xi_c + \lambda (\xi + \mathbf{H}_c^T \xi_c)$, as defined in Eq. 2. Specifically, \mathbf{u} denotes collective gradient ξ_c and \mathbf{v} denotes $(\xi + \mathbf{H}_c^T \xi_c)$.

We then extend the definition of infinitesimal alignment (Balduzzi et al., 2018) to our proposed AgA gradient. Given a third reference vector \mathbf{w} , the **infinitesimal alignment** for AgA gradient $\tilde{\xi}$ with \mathbf{w} is defined as

$$\text{align}(\tilde{\xi}, \mathbf{w}) := \frac{d}{d\lambda} \{ \cos^2 \theta_\lambda \}_{|\lambda=0}. \quad (3)$$

Intuitively, we may presume that vectors \mathbf{u} and \mathbf{w} are directionally aligned, given that $\mathbf{u}^T \mathbf{w} > 0$. In this scenario, $\text{align} > 0$ implies that vector \mathbf{v} is drawing \mathbf{u} closer towards the reference vector \mathbf{w} . Conversely, vector \mathbf{v} is propelling \mathbf{u} away from \mathbf{w} . Similar arguments hold for $\text{align} < 0$: \mathbf{v} pushes \mathbf{u} away from the reference vector \mathbf{w} when \mathbf{u} and \mathbf{w} share the same directional orientation. Conversely, \mathbf{v} pulls \mathbf{u} towards the reference vector \mathbf{w} when the vectors \mathbf{u} and \mathbf{w} are not oriented in the same direction.

The ensuing lemma provides a simplified method for determining the sign of align , circumventing the need for generating an exact solution.

Lemma A.1 (Sign of align). *Given AgA gradient $\tilde{\xi}$ and reference vector $\nabla \mathcal{H}_c$, the sign of infinitesimal alignment align could be calculated by*

$$\text{sign} \left(\text{align}(\tilde{\xi}, \nabla \mathcal{H}_c) \right) = \text{sign} \left(\langle \tilde{\xi}, \nabla \mathcal{H}_c \rangle (\langle \xi_c, \nabla \mathcal{H}_c \rangle + \|\nabla \mathcal{H}_c\|^2) \right).$$

Proof. By the definition of θ_λ , we could directly get:

$$\cos^2 \theta_\lambda \quad (4a)$$

$$= \left(\frac{\langle \tilde{\xi}, \nabla \mathcal{H}_c \rangle}{\|\tilde{\xi}\|^2 \cdot \|\nabla \mathcal{H}_c\|^2} \right)^2 \quad (4b)$$

$$= \left(\frac{\langle \xi_c + \lambda(\xi + \nabla \mathcal{H}_c), \nabla \mathcal{H}_c \rangle}{\|\tilde{\xi}\|^2 \cdot \|\nabla \mathcal{H}_c\|^2} \right)^2 \quad (4c)$$

$$= \frac{\langle \xi_c, \nabla \mathcal{H}_c \rangle^2 + 2\lambda \langle \xi_c, \nabla \mathcal{H}_c \rangle \langle \xi + \nabla \mathcal{H}_c, \nabla \mathcal{H}_c \rangle + \mathcal{O}(\lambda^2)}{\left(\|\tilde{\xi}\|^2 \cdot \|\nabla \mathcal{H}_c\|^2 \right)^2} \quad (4d)$$

$$= \frac{\langle \xi_c, \nabla \mathcal{H}_c \rangle^2 + 2\lambda \langle \xi, \nabla \mathcal{H}_c \rangle \langle \xi_c, \nabla \mathcal{H}_c \rangle + 2\lambda \|\nabla \mathcal{H}_c\|^2 \langle \xi_c, \nabla \mathcal{H}_c \rangle + \mathcal{O}(\lambda^2)}{\left(\|\tilde{\xi}\|^2 \cdot \|\nabla \mathcal{H}_c\|^2 \right)^2} \quad (4e)$$

$$= \frac{\langle \xi_c, \nabla \mathcal{H}_c \rangle^2 + 2\lambda \langle \xi_c, \nabla \mathcal{H}_c \rangle (\|\nabla \mathcal{H}_c\|^2 + \langle \xi, \nabla \mathcal{H}_c \rangle) + \mathcal{O}(\lambda^2)}{\left(\|\tilde{\xi}\|^2 \cdot \|\nabla \mathcal{H}_c\|^2 \right)^2}. \quad (4f)$$

In accordance with the established definition of infinitesimal alignment, it becomes feasible to further compute the sign of

align by taking the derivative of λ with respect to $\cos^2 \theta_\lambda$:

$$\text{sign} \left(\text{align}(\tilde{\xi}, \nabla \mathcal{H}_c) \right) \quad (5a)$$

$$= \text{sign} \left(\frac{d}{d\lambda} \cos^2 \theta_\lambda \right) \quad (5b)$$

$$= \text{sign} \left(\langle \xi_c, \nabla \mathcal{H}_c \rangle (\langle \xi, \nabla \mathcal{H}_c \rangle + \|\nabla \mathcal{H}_c\|^2) \right). \quad (5c)$$

□

Lemma A.1 empowers us to calculate the sign of infinitesimal alignment relying on components that are readily computable.

Let us observe $\langle \xi_c, \nabla \mathcal{H}_c \rangle = \xi_c^T \mathbf{H}_c \xi_c$ for symmetric Hessian matrix \mathbf{H}_c . Under the assumption of $\xi_c \neq 0$, we could derive:

$$\begin{cases} \text{if } \mathbf{H}_c \succeq 0, \text{ then } \langle \xi_c, \nabla \mathcal{H}_c \rangle \geq 0; \\ \text{if } \mathbf{H}_c \prec 0, \text{ then } \langle \xi_c, \nabla \mathcal{H}_c \rangle < 0. \end{cases} \quad (6)$$

As demonstrated by Eq. 6, when situated in the neighborhood of a stable fixed point (that is to say, $\mathbf{H}_c \succeq 0$), we observe $\langle \xi_c, \nabla \mathcal{H}_c \rangle \geq 0$. In converse circumstances, $\langle \xi_c, \nabla \mathcal{H}_c \rangle < 0$ occurs. Following this, we shall proceed to delve into two specific scenarios: stability and instability of the fixed point.

1) Case 1: In a neighborhood of a stable fixed point. If we are in a neighborhood of a stable fixed point then $\langle \xi_c, \nabla \mathcal{H}_c \rangle \geq 0$. This indicates that both vectors ξ_c and $\nabla \mathcal{H}_c$ point in the same direction, i.e., $\theta(\xi_c, \nabla \mathcal{H}_c) \leq \pi/2$. Referring to Lemma A.1, the sign of $\text{align}(\tilde{\xi}, \nabla \mathcal{H}_c)$ is the same as the sign of $\langle \xi, \nabla \mathcal{H}_c \rangle + \|\nabla \mathcal{H}_c\|^2$ if $\langle \xi_c, \nabla \mathcal{H}_c \rangle \geq 0$. Consequently, we have $\text{sign}(\lambda) = \text{sign}(\langle \xi, \nabla \mathcal{H}_c \rangle + \|\nabla \mathcal{H}_c\|^2) = \text{sign}(\text{align})$ matching the claim of our corollary.

Let us now conjecture the scenarios of $\text{sign}(\text{align})$, namely, $\text{sign}(\text{align}) \geq 0$ or $\text{sign}(\text{align}) < 0$. When $\text{sign}(\text{align}) \geq 0$, it follows that $\text{sign}(\lambda) \geq 0$. Consequently, vector v will draw u towards w . Subsequently, when $\text{sign}(\text{align}) < 0$, we observe that $\text{sign}(\lambda) < 0$. A negative λ reverses the mechanism such that v pushes u away from w , aligning with the discussion following Eq. 3 that assumes a positive λ . Thus, regardless of the sign of align , if we set $\text{sign}(\lambda) = \text{sign}(\langle \xi, \nabla \mathcal{H}_c \rangle + \|\nabla \mathcal{H}_c\|^2)$, vector v ensures u is drawn towards w .

From now, we prove that in the neighborhood of a stable fixed point, if we let $\text{sign}(\lambda)$ satisfy $\lambda \cdot \langle \xi_c, \nabla \mathcal{H}_c \rangle (\langle \xi, \nabla \mathcal{H}_c \rangle + \|\nabla \mathcal{H}_c\|^2) \geq 0$, the AgA gradient $\tilde{\xi}$ will be pulled more closer to $\nabla \mathcal{H}_c$ than ξ_c .

2) Case 2: In a neighborhood of an unstable fixed point. The proofing approach for the unstable case exhibits similarity to Case 1.

Therefore, we prove that if we let the sign of λ follows the condition $\lambda \cdot \langle \xi_c, \nabla \mathcal{H}_c \rangle (\langle \xi, \nabla \mathcal{H}_c \rangle + \|\nabla \mathcal{H}_c\|^2) \geq 0$, the optimization process using the AgA method exhibit following attributes. In areas close to fixed points, 1) if the point is stable, the AgA gradient will be pulled toward this point, which means that $\theta(\tilde{\xi}, \nabla \mathcal{H}_c) \leq \theta(\xi_c, \nabla \mathcal{H}_c)$; 2) if the point represents unstable equilibria, the AgA gradient will be pushed out of the point, indicating that $\theta(\tilde{\xi}, \nabla \mathcal{H}_c) \geq \theta(\xi_c, \nabla \mathcal{H}_c)$. An illustrative example of the corollary is provided in Fig. 2.

□

B. Additional Experiment Results

B.1. Result Visualization of Two-player Public Goods Game

Fig. 6 depicts the actions produced by various methods in a two-player public game. The action generated by each method is represented by a circle, which is color-coded according to the corresponding method. To ensure fairness, each method's updates are constrained to a maximum of 100 steps. These methods include the individual loss-driven simultaneous optimization (Simul-Ind), two variants of gradient adjustment methods termed as CGA and SGA, and the simultaneous optimization leveraging collective loss (Simul-Co) alongside our proposed AgA, where $\lambda = 1$. Each of these methods is fundamentally underpinned by the gradient ascent algorithm. The illustration consolidates data from 50 randomized runs initialized from diverse starting points. The 'X' demarcated circles indicate the average actions mapped to each method. From the figure, it's apparent that Simul-Ind, CGA, SGA, SVO tend to converge towards scenarios where at least one player

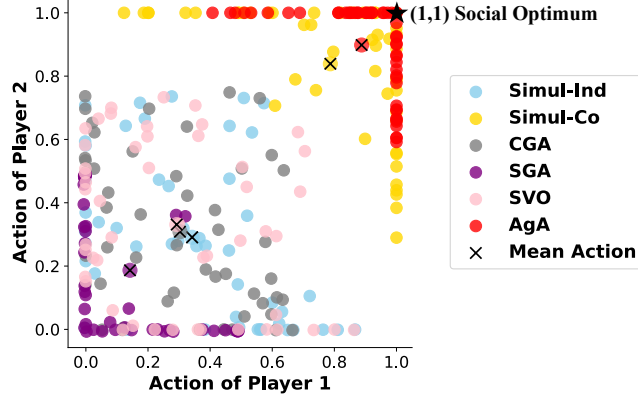


Figure 6. The scatter of actions in a two-player public goods game achieved through different optimization methods. Each circle represents the position attained within a maximum of 100 steps, with the color indicating the corresponding method. The 'X' mark represents the mean actions of 50 random runs. With the exception of Simul-Co, the baseline methods converge towards the Nash equilibrium (0,0). Notably, while both AgA and Simul-Co display altruistic behavior, the actions of AgA are more tightly clustered around the (1,1) point compared to Simul-Co.

abstains from contributing, an occurrence often tagged as ‘free-riding’. In contrast, Simul-Co (represented by a yellow circle) and our AgA method (illustrated as a red circle) tend to converge towards scenarios characterized by enhanced contributions or ‘altruism’. The observed results underline that players employing the AgA method exhibit heightened altruistic tendencies relative to those operating under Simul-Co. Further, AgA exhibits a superior alignment towards socially optimal outcome point (1, 1).

C. Experiment Details

C.1. Social Dilemma Games: Cleanup and Harvest

SSD games (Vinitsky et al., 2019) implements the Harvest and Cleanup as grid world games. The agents use partially observed graphics observation, which contains a grid of 15×15 centered on themselves. Compared to the original Cleanup and Harvest games, SSD games add a fire beam mechanic, where agents can fire on the grid to hit other partners. An agent will gain 1 reward if harvesting an apple and -1 reward if firing a beam. Besides, being hit by a beam will result in a 50 individual reward loss. Under this mechanic, selfish agents can easily use fire to prevent others from harvesting apples to gain more individual rewards but harm social welfare.

We utilized PPO algorithm in stable-baselines3 (Raffin et al., 2021) to implement the baselines and our methods, with all the agents using separated policy parameters for Simul-Ind and sharing same policy parameters for other experiments. For SVO, we modify the individual reward to be $r_i - \alpha(1 - \text{actan} \left(\frac{\sum_{j:j \neq i} r_j}{r_i} \right))$. To employ CGA and AgAs to PPO training process, we compute both individual and collective PPO-Clip policy losses and subsequently utilize them to calculate the adjusted gradient through automatic differentiation. We don’t make changes to the critic loss nor the critic net optimization process.

The hyper-parameters for PPO training are as follows.

- The learning rate is 1e-4
- The PPO clipping factor is 0.2.
- The value loss coefficient is 1.
- The entropy coefficient is 0.001.
- The γ is 0.99.
- The total environment step is 1e7 for Harvest and 2e7 for Cleanup.
- The environment episode length is 1000.

- The grad clip is 40.

C.2. Mixed-motive StarCraft II

SMAC, often employed as a testbed within the sphere of cooperative MARL, is characterized by the shared reward system among players. Within this paper, we present the MMM2 map transformed as a versatile testbed designed for mixed-motive cooperation. Specifically, MMM2 map encompasses 10 agents and 12 adversaries as enumerated below:

- Controlled Agents: Comprised of 1 Medivac, 2 Marauders, and 7 Marines.
- Adversaries: Incorporates 1 Medivac, 3 Marauders, and 8 Marines.

Moreover, this setting embodies both heterogeneity and asymmetry, where agents within the same team exhibit diverse gaming skills. Additionally, the team compositions, for instance, variation in agent number and type, differ in both opposing factions. Consequently, the intricate gaming mechanism, the presence of heterogeneous players, and the discernible asymmetry conspire to establish an exemplary milieu conducive for the exploration of mixed-motive issues.

In order to create a mixed-motive testbed, we adjusted the reward system hailing from the original SMAC environment. With this, we proposed a revamped reward function that features two distinct components: a reward for imposing damage and a penalty associated specifically with agent fatalities. In a move to potentially intensify internal conflicts amongst agents, the reward for imposing damage is solely allocated to the agent responsible for executing the attack on the enemy. Additionally, the death of an agent results in the imposition of an extra penalty. Consequently, this mechanism fosters an environment where agents are predisposed towards individual protection and separate reward acquisition, as opposed to collective cooperation.

Formally, the agent i 's reward at step t is defined as follows:

$$\text{delta-enemy}_i = \sum_{\substack{j \in \text{Enemy} \\ i \text{ hit } j \text{ at } t}} [(\text{previous-health} - \text{current-health}) + (\text{previous-shield} - \text{current-shield})]$$

The individual reward for Player i is determined as follows: If the player dies, then $r_i = \text{delta-enemy}_i - \beta \times \text{penalty}$; otherwise, if the player survives, then $r_i = \text{delta-enemy}_i$.

Experiment settings. Simul-Ind leverages IPPO with recurrent policies and distinct policy networks. Conversely, Simul-Co employs MAPPO with recurrent policies and consolidated policy networks. The implementation of the IPPO and MAPPO algorithms presented in this paper is founded on the methodology detailed in (Yu et al., 2022). We utilize gradient adjustment optimization methods, such as CGA and AgAs, derived from MAPPO, implementing gradient adjustments as outlined in Algorithm 1.

The hyper-parameters for PPO-based training are as follows.

- The learning rate is 5e-4
- The PPO clipping factor is 0.2.
- The value loss coefficient is 1.
- The entropy coefficient is 0.01.
- The γ is 0.99.
- The total environment step is 1e7.
- The factor β in reward function is 1.
- The environment episode length is 400.